Metal-binding polymorphism in late embryogenesis abundant protein AtLEA4-5, an intrinsically disordered protein

Leidys French-Pacheco[1], Cesar L. Cuevas-Velazquez[2], Lina Rivillas-Acevedo[3], Alejandra A. Covarrubias[2] and Carlos Amero[1]

[1] Centro de Investigaciones Químicas, IICBA, Universidad Autónoma del Estado de Morelos, Cuernavaca, Morelos, Mexico
[2] Departamento de Biología Molecular de Plantas, Instituto de Biotecnología, Universidad Nacional Autónoma de México, Cuernavaca, Morelos, Mexico
[3] Centro de Investigación en Dinámica Celular, IICBA, Universidad Autónoma del Estado de Morelos, Cuernavaca, Morelos, Mexico

ABSTRACT

Late embryogenesis abundant (LEA) proteins accumulate in plants during adverse conditions and their main attributed function is to confer tolerance to stress. One of the deleterious effects of the adverse environment is the accumulation of metal ions to levels that generate reactive oxygen species, compromising the survival of cells. AtLEA4-5, a member of group 4 of LEAs in *Arabidopsis*, is an intrinsically disordered protein. It has been shown that their *N*-terminal region is able to undergo transitions to partially folded states and prevent the inactivation of enzymes. We have characterized metal ion binding to AtLEA4-5 by circular dichroism, electronic absorbance spectroscopy (UV–vis), electron paramagnetic resonance, dynamic light scattering, and isothermal titration calorimetry. The data shows that AtLEA4-5 contains a single binding site for Ni(II), while Zn(II) and Cu(II) have multiple binding sites and promote oligomerization. The Cu(II) interacts preferentially with histidine residues mostly located in the C-terminal region with moderate affinity and different coordination modes. These results and the lack of a stable secondary structure formation indicate that an ensemble of conformations remains accessible to the metal for binding, suggesting the formation of a fuzzy complex. Our results support the multifunctionality of LEA proteins and suggest that the C-terminal region of AtLEA4-5 could be responsible for antioxidant activity, scavenging metal ions under stress conditions while the *N*-terminal could function as a chaperone.

Subjects Biochemistry, Biophysics, Plant Science
Keywords Intrinsically disordered proteins, Metal binding, Protein self-assembly, Fuzzy complex

INTRODUCTION

Late embryogenesis abundant (LEA) proteins are highly expressed and accumulated in plants during the dehydration stage of seeds and pollen, but also in response to water deficit conditions and to other adverse environments (*Dure et al., 1983*;

Battaglia et al., 2008; *Hand et al., 2011*). These characteristics have suggested that their main role is to confer tolerance to stress conditions (*Kovács, Agoston & Tompa, 2008*; *Hincha & Thalhammer, 2012*). LEA proteins are grouped in seven families (LEA1–LEA7) according to their sequence similarity, phylogeny, and characteristic motifs (*Battaglia et al., 2008*). Most of them are classified as intrinsically disordered proteins (IDPs), due in part to their high content of small, polar, and charged amino acids (*Garay-Arroyo et al., 2000*; *Battaglia et al., 2008*; *Olvera-Carrillo, Reyes & Covarrubias, 2011*; *Hincha & Thalhammer, 2012*). Experimental evidence by circular dichroism (CD) and nuclear magnetic resonance have confirmed large amounts of disordered conformations for some members (*Rivera-Najera et al., 2014*; *Cuevas-Velazquez et al., 2016*). However, in the presence of α-helix inducers as trifluoroethanol LEA proteins may undergo transitions to partially folded states. This phenomenon also occurs under dehydration and conditions that simulate low osmotic potentials or macromolecular crowding (*Soulages et al., 2002*; *Cuevas-Velazquez et al., 2016*; *Bremer et al., 2017*).

To promote tolerance of plants, they may act as chaperone-like proteins by interacting with other proteins to preclude the inactivation and subsequent aggregation that they experience under stress conditions (*Reyes et al., 2005*; *Chakrabortee et al., 2007*; *Kovács, Agoston & Tompa, 2008*; *Battaglia & Covarrubias, 2013*). There is also evidence indicating that some LEA proteins may be involved in the stabilization of biological membranes (*Koag et al., 2009*; *Bremer et al., 2017*) and in nucleic acids protection by direct interaction (*Hara et al., 2009*; *Saumonneau et al., 2012*). Furthermore, it has been reported that LEA proteins from different families are able to bind metals, suggesting a role as metal ion sequestering agents (*Krüger et al., 2002*; *Liu et al., 2011*; *Hara et al., 2016*).

In plants, metal ions can accumulate to levels that generate reactive oxygen species (ROS), compromising the survival of cells (*DalCorso et al., 2014*). ROS might be produced by free catalytic metal as Cu(II), Zn(II) or Fe(III) via the Haber–Weiss and the Fenton reactions or metabolic alterations (*Letelier et al., 2005*; *Ravet & Pilon, 2013*; *DalCorso et al., 2014*). The putative interaction of LEA proteins with metal ions suggests that they might prevent the deleterious effects caused by the accumulation of such molecules (*Hara, Fujinaga & Kuboi, 2004*; *Liu et al., 2011*). Previous works have reported interaction with Zn(II), Ni(II), Cu(II), and Fe(III), for CuCOR15 a member of group 2 from citrus (*Hara, Fujinaga & Kuboi, 2005*); ZmLEA3 a member of group 3 from maize (*Liu et al., 2013*) and GmPM1 and GmPM9 members of group 4 from soybean (*Liu et al., 2011*). Interestingly, GmPM1 and GmPM9 bind Fe(III) and Cu(II) but not Ca(II) or Mg(II) ions, and hence it is not clear if the metal binding and specificity is conserved in each group or if it is protein-specific.

In *Arabidopsis thaliana*, the group 4 of LEA proteins is formed by three basic and hydrophilic non-redundant proteins: AtLEA4-1, AtLEA4-2, and AtLEA4-5, that have been classified as IDPs (*Olvera-Carrillo et al., 2010*; *Shih et al., 2010*). Their amino terminal region is highly conserved, whereas their carboxyl terminal region is more variable, with 54.64% sequence identity between AtLEA4-1 and AtLEA4-2, 29.69% between AtLEA4-1 and AtLEA4-5 and 26.09% between AtLEA4-2 and AtLEA4-5 (Fig. 1). It has been shown that two members of this family, AtLEA4-5 and AtLE4-2, undergo transitions
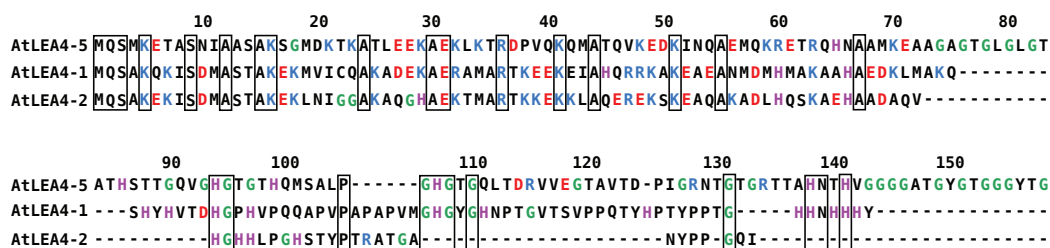
```
              10         20         30         40         50         60         70         80
AtLEA4-5 MQSMKETASNIAASAKSGMDKTKATLEEKAEKLKTRDPVQKQMATQVKEDKINQAEMQKRETRQHNAAMKEAAGAGTGLGLGT
AtLEA4-1 MQSAKQKISDMASTAKEKMVICQAKADEKAERAMARTKEEKEIAHQRRKAKEAEANMDMHMAKAAHAEDKLMAKQ--------
AtLEA4-2 MQSAKEKISDMASTAKEKLNIGGAKAQGHAEKTMARTKKEKKLAQEREKSKEAQAKADLHQSKAEHAADAQV-----------

              90        100        110        120        130        140        150
AtLEA4-5 ATHSTTGQVGHGTGTHQMSALP------GHGTGQLTDRVVEGTAVTD-PIGRNTGTGRTTAHNTHVGGGGATGYGTGGGYTG
AtLEA4-1 ---SHYHVTDHGPHVPQQAPVPAPAPVMGHGYGHNPTGVTSVPPQTYHPTYPPTG-----HHNHHHY---------------
AtLEA4-2 ----------HGHHLPGHSTYPTRATGA---------------------NYPP-GQI----------------------------
```

Figure 1 Sequence alignment for group 4 LEA proteins from *Arabidopsis thaliana*: AtLEA4-5, AtLEA4-1, and AtLEA4-2. According to the nomenclature of LEA proteins, numbers 1, 2, and 5 indicate the chromosome where their corresponding genes are localized. Fully conserved residues are contained in black boxes, positive charged residues are in blue, negative charged residues are in red, glycines are in green and histidines are in purple. Their amino terminal region is highly conserved, whereas their carboxyl terminal region is more variable, with 54.64% sequence identity between AtLEA4-1 and AtLEA4-2, 29.69% between AtLEA4-1 and AtLEA4-5, and 26.09% between AtLEA4-2 and AtLEA4-5.   Full-size ⬛ DOI: 10.7717/peerj.4930/fig-1

to partially folded states, mainly alpha helices as determined by CD, under conditions that mimic low osmotic potentials or high macromolecular crowding simulated by different concentrations of glycerol or polyethylene glycol, respectively (*Cuevas-Velazquez et al., 2016*). Also, both proteins prevent the inactivation and/or the aggregation of enzymes under partial dehydration or freeze-thaw treatments (*Reyes et al., 2008*; *Cuevas-Velazquez et al., 2016*). Previous analysis showed that besides the characteristic amino acid composition of typical LEA proteins, group 4 LEA proteins present a particular bias towards a high content of positively charged residues (Arg and Lys) in their amino terminal region, whereas their carboxy terminal region show a high percentage of Gly and His residues (Fig. 1) (*Cuevas-Velazquez, Reyes & Covarrubias, 2017*).

To gain insight into the properties of the Arabidopsis group 4 LEA proteins, we have characterized the metal binding by several biophysical techniques, such as CD, electronic absorbance spectroscopy (UV–vis), electron paramagnetic resonance (EPR), dynamic light scattering (DLS), and isothermal titration calorimetry (ITC). In this work, we show that AtLEA4-5 is able to bind Zn(II), Cu(II), and Ni(II) but not Ca(II), Mn(II), and Fe(III), and describe the metal binding properties for this protein.

MATERIALS AND METHODS

All reagents were analytic grade, and used without further purification. The water used was MQ grade. $CuCl_2$ and $CuSO_4$, $MnCl_2$, $FeCl_3$, $CaCl_2$, $NiSO_4$, and $ZnSO_4$ were used as source of Cu(II), Mn(II), Fe(III), Ca(II), Ni(II), and Zn(II) ions, respectively.

Protein expression and purification

The AtLEA4-5/pTrc99A plasmid was transformed into the *Escherichia coli* D3-lysS strain (*Cuevas-Velazquez et al., 2016*). Bacterial cells were grown in 1 L of LB, supplemented with 100 μg mL^{-1} ampicillin at 37 °C. The recombinant protein expression was induced by addition of 0.3 mM isopropyl-D-thiogalactopyranoside at $OD_{600} = 0.6$, and harvested by centrifugation after incubation during 6 h at 25 °C. The cell pellet was resuspended in 20 mM Tris–HCl, pH 7, 10 mM NaCl and lysed on ice by sonication.

AtLEA4-5 was purified by thermic treatment of the bacterial protein extract, followed by differential precipitation with trichloroacetic acid, as previously described (*Campos et al., 2011*).

Immobilized metal ion affinity chromatography

The interaction with metal ions was analyzed by immobilized metal ion affinity chromatography (IMAC) using 1 mL HiTrap chelating HP columns following manufacturer instructions (GE Healthcare Life Science, Princeton, NJ, USA).

The columns were charged with different metal ions by loading 5 mL of 100 mM of $MnCl_2$, $CaCl_2$, $FeCl_3$, $ZnSO$, $CuSO_4$ or $NiSO_4$, and washed with 10 mL of deionized water. Every column was equilibrated with 50 mM Tris–HCl pH 7.5, 1M NaCl, except the one that contains $FeCl_3$, which was equilibrated at 50 mM Tris–HCl pH 5.5. A total of 50 μM of protein was loaded into the columns and then washed with 8 mL of 50 mM Tris–HCl pH 7.5, 1M NaCl. The bound protein was eluted with 4 mL of 50 mM Tris–HCl pH 7.5, 1M NaCl 250 mM Ethylenediaminetetraacetate acid (EDTA). Every fraction was analyzed by Sodium dodecyl sulfate polyacrylamide (SDS–PAGE).

UV–visible absorption

Electronic absorption spectra were acquired on an Agilent 8453 UV–visible diode array spectrophotometer at room temperature. AtLEA4-5 protein samples were 120 μM in either 10 mM PBS, pH 7.5 or 10 mM NEM (4-ethylmorpholine) pH 7.5. Titration steps of 0.5 equivalents of metal ions were used to analyze the formation of protein-metal complexes. Changes were observed between 200 and 800 nm. Duplicates experiments were performed for each condition. NEM buffer was chosen due to its non-chelating properties (*Garnett & Viles, 2003*).

Circular dichroism

The formation of the metal-protein complex was monitored by CD in the presence of metal ions. Spectra were acquired on a Jasco J-815 CD spectropolarimeter, using a 1 cm path length quartz cuvette at room temperature. A 120 μM AtLEA4-5 sample in 10 mM NEM, pH 7.5 was titrated by the addition of 0.5 equivalents of $CuSO_4$.

Secondary structure changes induced by the protein-metal ion interaction were followed by the addition of increasing amounts of metal ions. The spectra in the far UV region (200–250 nm) were recorded at each titration point. Duplicates experiments were performed for each condition.

Electron paramagnetic resonance

Paramagnetic resonance spectra were collected in the X-band microwave frequency (9.5 GHz) using an EMX Plus Bruker System, at 150 K with a ER4131VT variable temperature nitrogen system. The samples were run using 10 mW microwave power, 5 G modulation amplitude, 100 kHz modulation frequency, 327 ms time constant, and 82 ms conversion time. AtLEA4-5 samples were 120 μM in 10 mM NEM, pH 7.5 and progressively increasing equivalents of $CuSO_4$ metal ions were added. Duplicates experiments were performed for each condition.

Absorption binding calculation

To get an estimation of the binding affinity, the average EPR signal from $g = 2.12$ and $g = 2.45$ were plotted as a function of Cu(II) concentration. The normalized values were analyzed by non-linear fitting using a hyperbolic equation:

$$y = \frac{p[\text{Cu}]}{(k_\text{b} + [\text{Cu}])}$$

where y is the absorbance, $[\text{Cu}]$ is the copper concentration, p is the maximum specific binding, and k_b is the apparent binding constant.

Isothermal titration calorimetry

Isothermal titration calorimetry experiments were performed at 25 °C on a Malvern ITC200 instrument. A total of 50 μM AtLEA4-5 in NEM 10 mM pH 7.5 was loaded into the sample cell and 1–4 mM of metal ion ($CuCl_2$, $ZnSO_4$ or $NiSO_4$) solution was loaded into the syringe. Each experiment consisted of 20 injections of 2 μL of each metal ion with 180 s interval between injections and stirring at 750 rpm. The heat of dilution was determined by making identical injection in the absence of protein. The net reaction heat was obtained by subtracting the heat of dilution from the corresponding total heat of reaction. Triplicate experiments were performed for each condition with different parameters.

The thermograms were integrated with the NIPTIC software package (*Keller et al., 2012*). The baseline, the beginning and the end of each peak were adjusted automatically by the program. Then the data sets were fitted using a nonlinear least-squares algorithm to a binding model of either one or multiple sets of non-interacting binding sites by SEDPHAT (*Zhao, Piszczek & Schuck, 2015*). The binding enthalpy change ΔH, and the association constant Ka were permitted to float during the least-squares minimization process and taken as the best-fit values.

Dynamic Light Scattering

Dynamic light scattering measurements were performed on a Malvern Zetasizer Nano ZSP spectrophotometer, with a scatter angle of 173°. AtLEA4-5 samples were 120 μM in 10 mM NEM, pH 7.5 in the absence and presence of 1, 2, 3 or 4 $CuCl_2$ equivalents. Samples with 50 and 12 μM were also used. The data were used to obtain translational diffusion coefficients through measurement of the decay rates of scattered light (correlation function) (*Stetefeld, McKenna & Patel, 2016*). The hydrodynamic radius, R_H, were obtained from the diffusion coefficients, D, via the Stokes–Einstein equation:

$$R_\text{H} = \frac{K_\text{B}T}{6\pi\eta D}$$

where K_B is Boltzmann's constant, T is the temperature, and η is the viscosity of the solution. We use 0.8872 cP for the viscosity at 25 °C. Typically, five runs with 10 scans of 10 s were obtained for each sample by triplicated. Data were analyzed by the cumulan and

the distribution methods implemented in the SEDPHAT/SEDFIT software (*Zhao, Piszczek & Schuck, 2015*; *Brautigam et al., 2016*).

An estimated hydrodynamic radius, R_H, for IDPs was calculated using (*Tomasso et al., 2016*):

$$R_H = (1.24 \times F_{PRO} + 0.904) \times (0.00759 \times |Q| + 0.963) \times 2.49 \times N^{0.509}$$

where N is the residue number, F_{PRO} is the fractional number of proline residues, and $|Q|$ is the absolute net charge determined from the sequence.

RESULTS

AtLEA4-5 was predicted to be disordered based on previous amino acid sequence analysis, while CD spectra showed a typical spectrum for a disorder protein, as indicated by the presence of minimum at ~200 nm (Fig. S1), in agreement with previous reports (*Cuevas-Velazquez et al., 2016*). In order to determine qualitatively if AtLEA4-5 was able to bind metal ions, IMAC was used. The elution of AtLEA4-5 through the metal-bound columns with different metal ions was followed by SDS–PAGE. For Ca(II), Mn(II), and Fe(III) columns, the protein was found in the washed fraction, indicating that the protein did not bind these metal ions (Fig. S2). For Zn(II), Cu(II), and Ni(II) columns, the protein was eluted only when EDTA was added, showing that the protein is able to bind these metal ions (Fig. S2).

Metal binding does not induce a change on secondary structure

To determine whether the metal-ion binding to AtLEA4-5 protein induces secondary structure formation, AtLEA4-5 protein samples containing increasing amounts of Cu(II), Zn(II), and Ni(II) were analyzed by CD. CD analysis by the CAPITO (*Wiedemann, Bellstedt & Görlach, 2013*) revealed a pre-molten globule like-state (Figs. S1 and S3). This profile did not undergo any significant variation after the addition of Cu(II), Zn(II), and Ni(II), suggesting that none of the metal ions tested induces changes in AtLEA4-5 secondary structure under these conditions (Fig. 2 and Fig. S3).

Histidine residues coordinate the binding to Cu(II)

Taking advantage of the paramagnetic properties of Cu(II), to further characterize the nature of the Cu(II) coordination to AtLEA4-5 we used electronic absorption (UV–vis and CD) in the UV–visible region. For this analysis AtLEA4-5 was titrated with different Cu(II) concentrations and the samples were analyzed. A negative band around 17,000 cm^{-1} ($\Delta\varepsilon = -1.98$) corresponding to a d–d transition was observed by CD. Moreover, three ligand to metal charge transfer (LMCT) bands were detected, two positive: 29,300 cm^{-1} ($\Delta\varepsilon = 0.33$) and 38,700 cm^{-1} ($\Delta\varepsilon = 1.05$), and one negative: 33,500 cm^{-1}, ($\Delta\varepsilon = -0.56$) (Fig. 3). The positive bands correspond to transitions from histidine imidazole group to copper, $\pi_1 \rightarrow$ Cu(II) (27,000–35,700 cm^{-1}) and $\pi_2 \rightarrow$ Cu(II) (32,500–40,800 cm^{-1}), whereas the negative band corresponds to a transition from deprotonated amides to the metal, N $\rightarrow$ Cu(II) (31,000–34,000 cm^{-1}) (*Bryce, Roeske & Gurd, 1966*; *Bernarducci et al., 1981*). These results indicate that
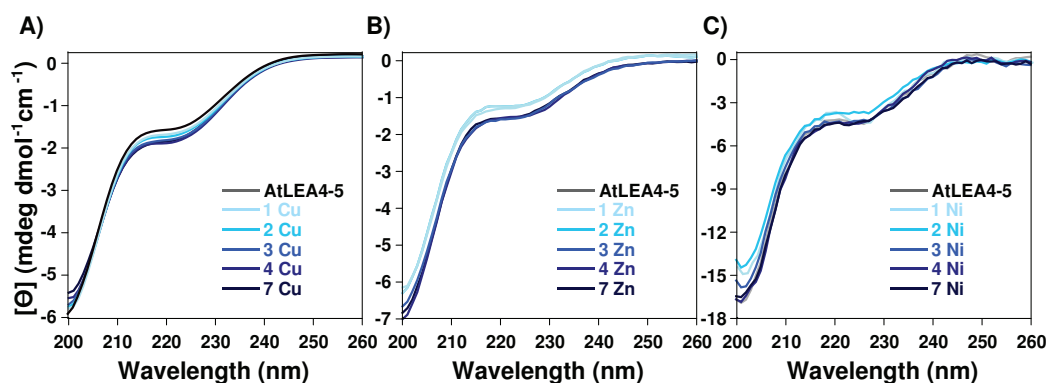
Figure 2 Effect of metal ions on AtLEA4-5 secondary structure. CD spectra of AtLEA4-5 titrated with (A) Cu(II), (B) Zn(II) and (C) Ni(II). Spectra of AtLEA4-5 in the absence (black line) or presence of 1, 2, 3, 4, and 7 equivalents of the metal ion (light to dark blue). The profiles did not undergo any significant variation after the addition of Cu(II), Zn(II) or Ni(II), suggesting that none of the metal ions induce changes in the AtLEA4-5 secondary structure under these conditions.

Full-size 🖼 DOI: 10.7717/peerj.4930/fig-2

AtLEA4-5 coordinates Cu(II) through at least one nitrogen of a histidine imidazole and backbone deprotonated amides.

Electron paramagnetic resonance spectroscopy was used to detect molecular changes produced by the local environment of paramagnetic Cu(II). With the addition of one equivalent of Cu(II), the EPR spectra showed two sets of signals: $g_{ll} = 2.2177/A_{ll} = 188.5$, and $g_{ll} = 2.261/A_{ll} = 182$, corresponding to a 4N and N3O equatorial coordination mode, respectively, according to the Peisach and Blumberg plots (*Peisach & Blumberg, 1974*). The splitting of the signal in the perpendicular region (~2.05) is also characteristic of a nitrogen coordination (Fig. 4) (*Nunes et al., 2010*). These results indicate that there are at least two species of the Cu(II)-AtLEA4-5 complex with two different equatorial coordination modes. The first with four nitrogen molecules, at least one from the imidazole of a histidine residue, while the others arise from the protein backbone deprotonated amides. The second mode involves one nitrogen, possibly from a histidine imidazole, and three oxygen molecules from protein carbonyl groups or from water molecules.

We estimated the binding parameters by plotting average EPR signals changes as function of Cu(II) concentrations. The data was fitted with to a hyperbolic equation and provided an apparent metal binding dissociation constant in the micromolar range (~300 μM) (Fig. S4).

Metal binding induces oligomerization

Even though, we did not find an effect of metal binding on AtLEA4-5 secondary structure, it was possible that this could affect its quaternary organization. In order to get insight of the oligomeric state of the metal complex, we perform DLS (Fig. 5 and Fig. S5). Although it is difficult to obtain an absolute size from an IDP, we can measure the diffusion coefficient and estimate the radius of a spherical molecule with that diffusion. As a reference, we used an empirical equation proposed to estimate the hydrodynamic
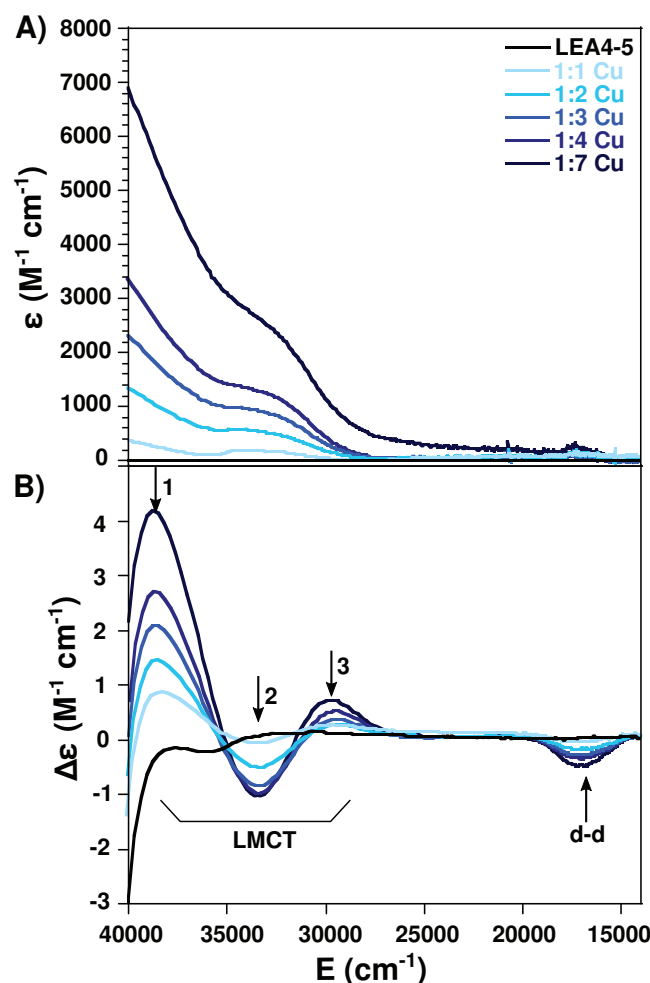
Figure 3 Cu(II)-AtLEA4-5 complex formation by electronic absorption. (A) UV–vis and (B) CD spectra of AtLEA4-5 in the absence (black line) or presence of 1, 2, 3, 4, and 7 equivalents of Cu(II) (light to dark blue). The arrows indicate the three ligand to metal charge transfer (LMCT) bands and the *d–d* bands. These bands correspond to transitions from the histidine imidazole group to copper and backbone deprotonated amides to copper. 　　　　　　　　　　　　Full-size ☑ DOI: 10.7717/peerj.4930/fig-3

radius from IDPs and calculated the corresponding translational diffusion coefficient ($R_H = 3$ nm, $D = 8.2 \times 10^{-7}$ cm^2 s^{-1}) for a monomer. The cellular concentration of LEA proteins is difficult to determine, due to the fact that they are differentially expressed during embryo-genesis and in response to water deficit (*Olvera-Carrillo, Reyes & Covarrubias, 2011*); nevertheless, a concentration of ~250 μM has been reported (*Roberts et al., 1993*). The DLS measurements of AtLEA4-5 solution at 120 μM concentration show a polydisperse curve, from were could obtain three mayor components with apparent diffusion coefficient of $D = 8.26 \times 10^{-6}$, $D = 1.95 \times 10^{-7}$, and $D = 0.07 \times 10^{-7}$ cm^2 s^{-1} which corresponds to apparent R_H of 2.98, 12.6, and 351 nm (Fig. S5). From this we could conclude that under these conditions AtLEA4-5 consist of different states, that include monomer, probably tetramers, and higher order oligomers. Lower protein concentration still result in polydisperse curves (Fig. S6). Different
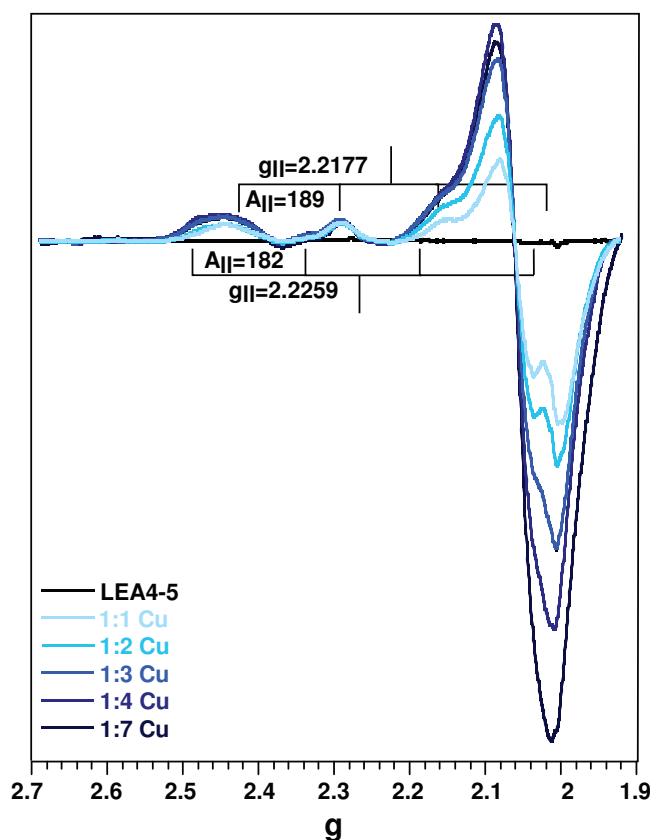
Figure 4 Cu(II)-AtLEA4-5 complex formation by EPR. EPR spectra of AtLEA4-5 in the absence (black line) or presence of 1, 2, 3, 4, and 7 equivalents of Cu(II) (light to dark blue). Two sets of signals were measured with $g_{ll} = 2.2177$ and $A_{ll} = 188.5$ and $g_{ll} = 2.261$ and $A_{ll} = 182$, corresponding to a 4N and N3O equatorial coordination, respectively. These results indicate that there are at least two species of the Cu(II)-AtLEA4-5 complex with two different equatorial coordination modes.

Full-size 🖼 DOI: 10.7717/peerj.4930/fig-4

oligomeric states in solution have already been reported for some other LEA proteins (*Rivera-Najera et al., 2014*; *Liu et al., 2017*).

Although it is difficult to correlate the diffusion coefficient with the absolute size of the protein, it can be used reliably to reveal changes due to an oligomerization process. DLS measurements of AtLEA4-5 in the presence of different Cu(II) concentration yielded a decrease in the translational diffusion coefficient consistent with a size increase due to oligomerization induced by metal binding (Fig. 5). The diffusion coefficient obtained for the metal complexes described by one average population (cumulant method, Fig. S5) were: $D = 0.134 \times 10^{-6}$ cm^2 s^{-1} 1:1 stoichiometry, $D = 0.1 \times 10^{-6}$ cm^2 s^{-1} 1:2 stoichiometry, $D = 0.06 \times 10^{-6}$ cm^2 s^{-1} 1:3 stoichiometry, and $D = 0.03 \times 10^{-6}$ cm^2 s^{-1} 1:4 stoichiometry (Fig. S5). All of theses states would correspond to higher order oligomers.

AtLEA4-5 presents moderate affinity for metal ions

Because IMAC procedure just yields qualitative information on proteins binding metal ions, we used ITC to obtain affinity values for the binding of AtLEA4-5 to Cu(II), Zn(II),
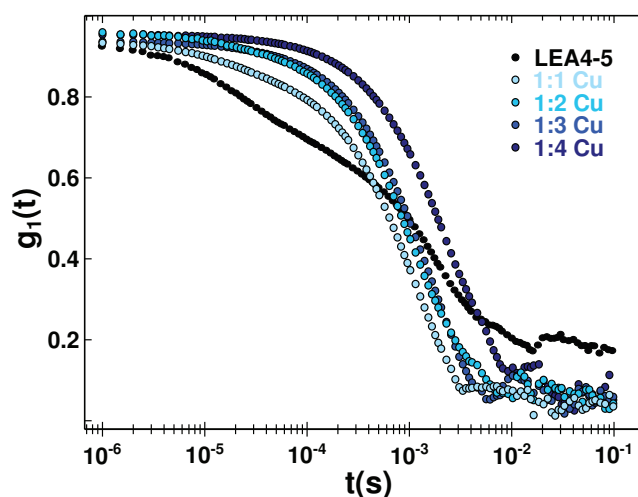
Figure 5 Protein oligomerization induced by metal binding. Correlation function of AtLEA4-5 in the absence (black line) or presence of 1, 2, 3, and 4 equivalents of Cu(II) (light to dark blue). The data were used to obtain translational diffusion coefficients by the cumulant and distribution methodologies (Fig. S5). Measurements of AtLEA4-5 in the presence of different Cu(II) concentrations yielded a shift to the right, indicating a size increase due to oligomerization induced by metal binding.

Full-size 🖼 DOI: 10.7717/peerj.4930/fig-5

and Ni(II). As shown in Fig. 6, the addition of Ni(II) produced a simple exothermic thermogram, which was best fitted to a single binding site model with a 1:1 stoichiometry; whereas the addition of Cu(II) and Zn(II) exhibited a complex behavior involving both exothermic and endothermic processes. At low equivalents of Cu(II) and Zn(II) the thermogram shows an exothermic heat reaction, which was followed by a late endothermic process as the metal concentration increases. This transition indicates the presence of at least two processes accounting for the different heat reactions (Fig. 6).

The resulting injection heats were fit with a binding model to estimate the binding affinity (K) and the enthalpy changes (ΔH). Whereas the free energy changes (ΔG) and the entropy changes (ΔS) were calculated by:

$$\Delta G = RT\ln K \text{ and } \Delta G = \Delta H - T\Delta S$$

where R is the gas constant (1.987 cal Kmol^{-1}) and T is the temperature in Kelvin (298 K).

In all cases, the negative enthalpies and the positive entropies for the first binding event (Table 1), indicated that the metal ion binding is enthalpic and entropic driven. In contrast, the positive ΔH and ΔS values for the endothermic reaction indicated a entropy-driven process. The largest apparent dissociation constants of AtLEA4-5 for each metal are in the micromolar range (Table 1) with a slightly higher affinity for Cu(II).

DISCUSSION

Ion sequestration by LEA proteins has been proposed as one of the possible functions in response to environmental stress such as cold, drought and high salinity (*Krüger et al., 2002*; *Hara, Fujinaga & Kuboi, 2004*; *Liu et al., 2011*, *2013*). Most of the evidence comes from IMAC screening experiments and from antioxidant activity assays
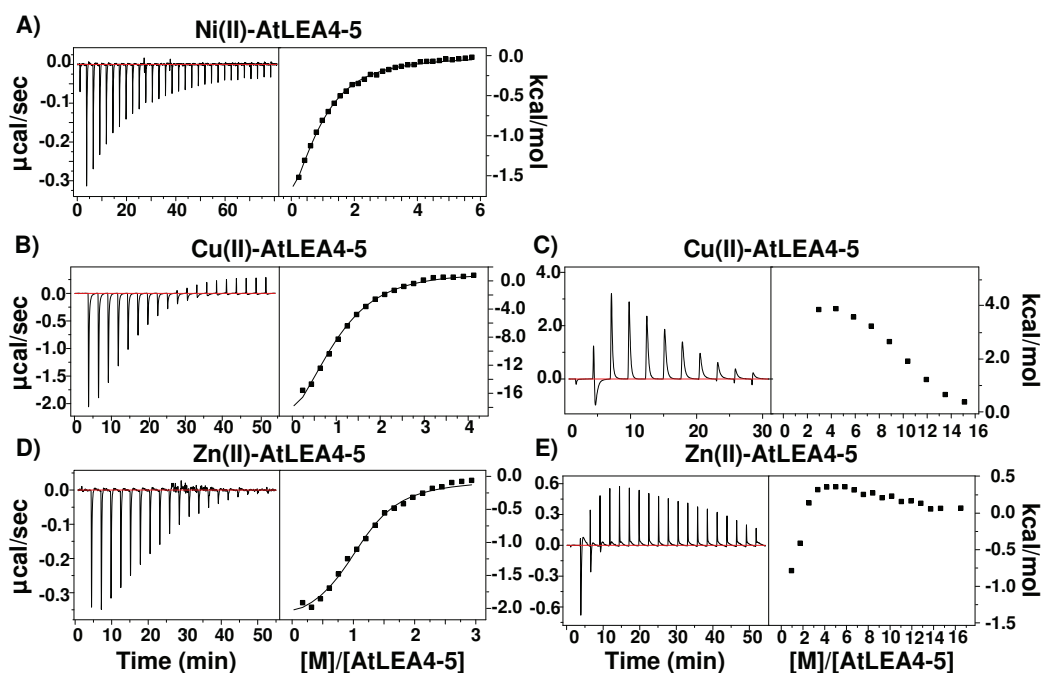
Figure 6 Metal binding by ITC. Isothermal titration calorimetry of AtLEA4-5 bound to (A) Ni(II), (B) Cu(II), and (C) Zn(II). The left side shows the experimental isothermic titrations; while the right side shows the reaction heat. In all cases the solid line represents the best fit to a binding model. (A) Ni(II) was best fitted to a single binding site model with a 1:1 stoichiometry. (B) and (C) Cu(II) and (D) and (E) Zn(II) exhibited a complex behavior involving both exothermic and endothermic processes and were fitted to multiple binding sites models. These transitions indicate the presence of at least two processes accounting for the different heat reactions. Full-size 🖼 DOI: 10.7717/peerj.4930/fig-6

(*Hara, Fujinaga & Kuboi, 2005*; *Liu et al., 2013*; *Hara et al., 2016*). However, little is known about the characteristics of the interaction between these proteins and metal ions; such as the association affinity, the regions and residues involved, their thermodynamic properties and the effect on the protein structural organization.

In this work, we report that AtLEA4-5, an Arabidopsis group 4 LEA protein, is able to bind Cu(II), Zn(II), and Ni(II), but not Ca(II), Mn(II), or Fe(III) (Fig. S2). The binding affinities, determined by ITC, are in the micromolar range which is comparable to previously reported values for proteins involved in metal sequestering as metallothioneins or phytochelatins (*Chekmeneva et al., 2008*; *Liu et al., 2011*), suggesting that AtLEA4-5 protein may play a role as metal detoxification, and as modulator of cell ion homeostasis during water deficit. Our results also indicated that AtLEA4-5 protein contains a single binding site for Ni(II), while Zn(II) and Cu(II) have multiple binding sites and promote oligomerization.

The data reported here showed that metal-protein complex formation does not induce a change in the protein secondary structure (α-helix or β-sheet) (Fig. 2; Fig. S3), and hence the protein probably is just forming loops mediated by the metal or multiple protein molecules are binding the same metal. In contrast to the classical binding paradigm for globular protein, the lack of a stable secondary structure formation and the moderate affinity, suggests that an ensemble of conformations remains accessible to the

Table 1 Thermodynamic parameters obtained from ITC analysis to characterize the binding between AtLEA4-5 protein and Cu(II), Zn(II), and Ni(II).

Metal ion	n site	K_a (L/mol)	K_d (μ mol/L)	ΔH (kcal/mol)	ΔS (cal/mol/deg)	ΔG (kcal/mol)
Cu(II)	1	$2 \times 10^5 \pm 3 \times 10^4$	6.4 ± 0.3	-20.7 ± 0.3	45.3	-7.2
	2	$6 \times 10^3 \pm 1 \times 10^2$	179 ± 0.01	-9.2 ± 0.7	13.8	-5.1
	3	$5 \times 10^5 \pm 3 \times 10^4$	1.8 ± 0.3	-32.9 ± 0.6	84.5	-7.7
Zn(II)	1	$9 \times 10^5 \pm 8 \times 10^5$	3.3 ± 1.25	-2.1 ± 0.04	-20.1	-8.1
	2	$3 \times 10^4 \pm 4 \times 10^3$	40 ± 25	-2.8 ± 0.4	-11.0	-6.1
Ni(II)	1	$3 \times 10^5 \pm 2 \times 10^4$	9.1 ± 0.5	-13.9 ± 0.2	-23.5	-6.9

metal for binding, favoring different types of metal association to specific protein sites. The formation of multiple binding modes with moderate affinity has been reported for other metal binding IDPs (*Chekmeneva et al., 2008*; *Liu et al., 2011*; *Sacco et al., 2012*).

It has been suggested that histidine residues could be the putative anchoring site for metal binding (*Gusman et al., 2001*). On this regard, AtLEA4-5 has a high content of histidines (1 in the *N*-terminal domain and 6 in the C-terminal domain). Moreover, electronic absorption (UV–vis and CD) data showed LMCTs characteristics of imidizole groups. Whereas EPR results indicate that there are at least, two coordination modes between the protein and Cu(II). The first one includes four nitrogen atoms which bind equatorially to Cu(II), at least one from a histidine imidazole, and the others from backbone deprotonated amides. While the second coordination mode includes one nitrogen, possibly from a histidine's imidazole, and three oxygens from backbone carbonyl group or water molecules (*Bernarducci et al., 1981*). The presence of a broad band from 540 to 650 nm in the CD spectra is also consistent with a mixture of species with different coordination modes (*Nunes et al., 2010*).

Self-assembly induced by metal ion binding has been reported for other IDPs such as alpha-synuclein (*Uversky, Li & Fink, 2001*), prion (*Bocharova et al., 2005*), Tau (*Mo et al., 2009*), and Aβ(1–42) peptide (*Bonda et al., 2011*; *Breydo & Uversky, 2011*). As indicated by DLS data, a similar behavior was observed for AtLEA4-5, with a decrease in the diffusion coefficient as Cu(II) concentration increased, implying the formation of oligomers mediated by metal binding. Recently, it has been shown for GmPM1, a LEA4 group member from soybean, that metal binding induces oligomerization probably involving His residues as detected by chemical cross-linking (*Liu et al., 2017*). Even though the role in planta of this metal binding effect on LEA protein structural organization is unknown, this may be related to a different mechanism to enforce their function as protectors of macromolecules or cellular structures, and/or as water organizers under extreme low water availability, as it occurs in dry seeds or in dehydrated resurrection plants, conditions where consequently metal concentrations tend to increase (*Otegui, 2002*; *Kranner & Colville, 2011*). This effect may also constitute a mechanism for LEA proteins to act as metal detoxifiers.

Interestingly, GmPM1 proteins bind Fe(III) (*Liu et al., 2011*), whereas we could not detect binding of AtLEA4-5 to this metal ion. The sequence similarity between AtLEA4-5

French-Pacheco et al. (2018), *PeerJ*, DOI 10.7717/peerj.4930

12/19

and GmPM1 is about 58% containing both of them several His residues (Fig. S7). And while both proteins are able to bind Cu(II), they differ in the binding capabilities for Fe(III). This suggests that, even though, many LEA proteins could be able to bind metal ions and form oligomers, there is not necessarily a conserved specificity for metal ion binding among LEA proteins, even from the same group. The different ion binding properties have to be further study to understand the relation to plant survival.

To gain insight into the thermodynamic of metal ion binding, we performed ITC experiments. This approach allows to directly measure the enthalpy changes, and obtain the association constants by a least-squares fit to a binding model. Then we calculate the free energy and the entropy changes. Ni(II) binding to AtLEA4-5 presents a single exothermic transition with a stoichiometric equivalence of 1:1, suggesting one binding site. Whereas, the thermograms obtained by the titration of Zn(II) and Cu(II) showed a complex process with an initial exothermic event followed by a late endothermic reaction (Fig. 6). The analysis of this type of curves is complicated due to the fact that it reflects contributions from different process.

Taking into consideration the spectroscopic data, that showed that AtLEA4-5 is able to bind several equivalents of metal in at least two different configurations, and that the metal binding induces the formation of oligomeric species, the thermogram must arise from a complicated interplay between the coordination chemistry of metal binding and the induced self-association. Based on this qualitative assessment, the binding isotherm was fitted to a multiple process model.

Even-though, the complexity of the process prevents us from completely dissecting the different contributions of the measured data, we can assume that the first exothermic event is describing the metal binding while the following events correspond to a mixture of subsequent metal ion binding and oligomerization. The observed favorable enthalpy in the first event, primarily reflects protein metal ion interactions, whereas the change in the binding entropy is related to metal ion desolvation. The following process is entropically controlled, which is likely due to the rearrangement of water surrounding the proteins and disruption of the metal ion hydration sphere upon metal binding and oligomerization.

While the ITC measures the enthalpy changes for any process (binding and oligomerization), the spectroscopic data are only sensitive to the metal binding and not to the oligomerization. Therefore, we used the EPR signals from the metal titration to estimate an apparent dissociation constant. The binding information obtained by the spectroscopy values is consistent with the ITC data with an apparent Kd binding in the µM range (Fig. S4). Under normal conditions, the metal ions concentration in plants has been reported in a low micromolar range (Álvarez-Fernández et al., 2014), suggesting a plausible physiologically relevant interaction between AtLEA4-5 and metal ions.

Previous reports have suggested that plants with silenced LEA 4 genes increase their susceptibility to oxidative stress (Senthil-Kumar & Udayakumar, 2006). This evidence, together with our results, particularly for Cu(II), suggests that AtLEA4-5 protein could have a protective role under oxidative stress. The Cu-AtLEA4-5 complex can act as a redox center, and consequently it may be responsible for antioxidant activity, scavenging
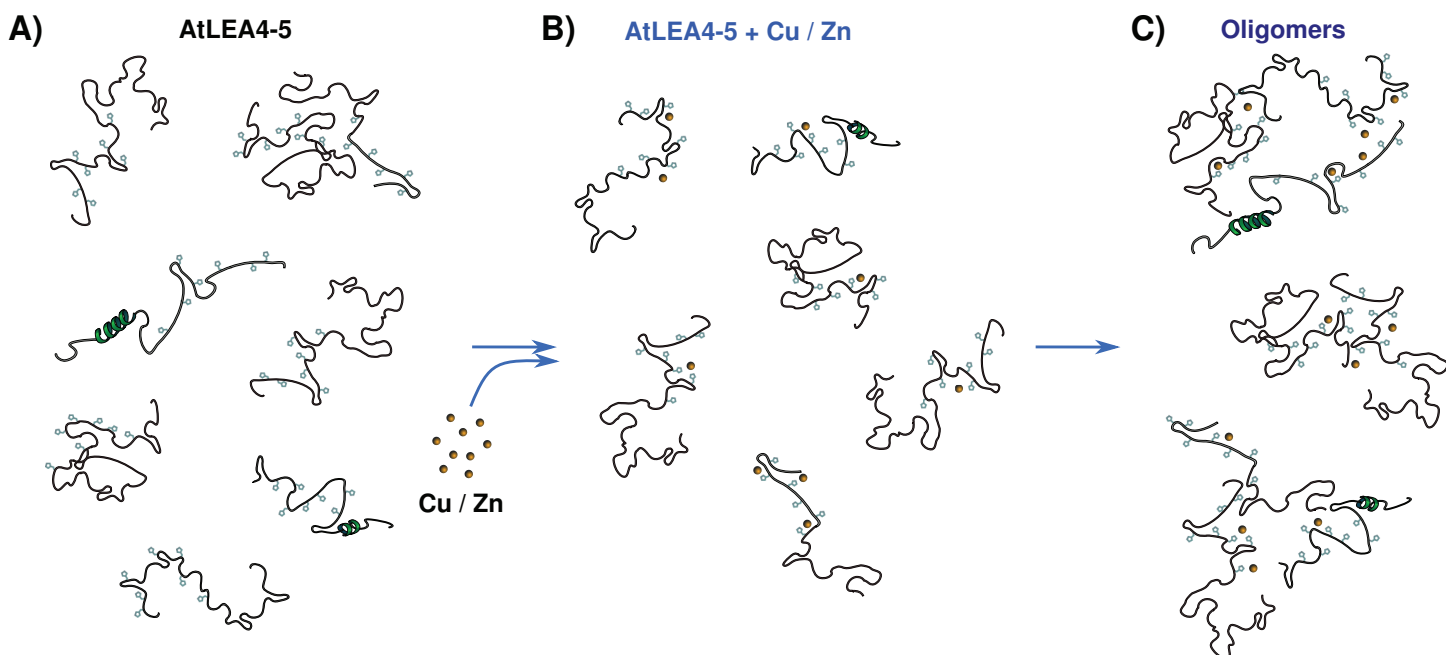
Figure 7 **Metal binding model.** (A) An ensemble of conformations is accessible for binding. (B) Metals interact with moderate affinity mainly with His residues, with multiple forms and multiple binding sites, without forming a unique well-defined binding site. (C) As metal ion concentration increases their binding to the protein induces the formation of oligomeric species. Full-size 🖼 DOI: 10.7717/peerj.4930/fig-7

metal ions or ROS under various stress conditions (*Liu et al., 2013*; *Hara, Kondo & Kato, 2013*). Due to the fact that all these proteins accumulate under water deficit conditions, these observations also could indicate that one of the deleterious effects of this adverse environment is the accumulation of metal ions, and that LEA proteins not only prevent the impairment of functional protein structures but also are able to counteract the detrimental outcome of metal ion increasing concentrations in cells. Metal ions accumulation could causes damage to metabolism, genetic expressions and structure of proteins. Also, physiological changes such as size and mass reductions has been reported when plants are treated with metals in the micro–millimolar range (*Kranner & Colville, 2011*).

Taking into account that the *N*-terminal region of AtLEA4-5 was able to fold and prevent enzyme unfolding, and that most of the His residues are located in the *C*-terminal region, it seems reasonable to think that while the amino terminal region could be responsible for protecting enzymatic activity by binding and adopting secondary structure features, the carboxy terminal region participates in metal sequestration reducing the generation of ROS.

CONCLUSION

The data presented here allow us to propose a metal binding model, where the ensemble of conformations remains accessible upon binding (Fig. 7). The metals interact mainly with His residues with moderate affinity in different conformations and multiple binding sites. These different coordination modes, without forming a unique well-defined binding site,

may indicate a fuzzy complex. A clouds-interaction model between IDPs and small-molecule ligands has been proposed (*Jin et al., 2013*); however, in this case it seems that the metal ions binds preferentially to His residues which, upon an increase in metal ion concentration, induces the formation of higher oligomeric species.

Our results support the multifunctionality of LEA proteins and suggest that the AtLEA4-5 protein might perform both protection roles, preventing loss of protein activity and metal scavenger under low water conditions shedding light on the functions of group 4 LEA proteins. The exact number and sequence of each binding site and the corresponding affinities is still to be determined.

ACKNOWLEDGEMENTS

ADDITIONAL INFORMATION AND DECLARATIONS

Funding

Grant Disclosures

Competing Interests

The authors declare that they have no competing interests.

Author Contributions

- Leidys French-Pacheco conceived and designed the experiments, performed the experiments, analyzed the data, prepared figures and/or tables, authored or reviewed drafts of the paper, approved the final draft.
- Cesar L. Cuevas-Velazquez performed the experiments, contributed reagents/materials/analysis tools, authored or reviewed drafts of the paper, approved the final draft.
- Lina Rivillas-Acevedo conceived and designed the experiments, performed the experiments, analyzed the data, authored or reviewed drafts of the paper, approved the final draft.
- Alejandra A. Covarrubias conceived and designed the experiments, contributed reagents/materials/analysis tools, authored or reviewed drafts of the paper, approved the final draft.

- Carlos Amero conceived and designed the experiments, analyzed the data, contributed reagents/materials/analysis tools, prepared figures and/or tables, authored or reviewed drafts of the paper, approved the final draft.

Data Availability

The following information was supplied regarding data availability:

The raw data are provided in the Supplemental Files.

Supplemental Information

Supplemental information for this article can be found online at http://dx.doi.org/10.7717/peerj.4930#supplemental-information.

REFERENCES

Álvarez-Fernández A, Díaz-Benito P, Abadía A, López-Millán AF, Abadía J. 2014. Metal species involved in long distance metal transport in plants. *Frontiers in Plant Science* **5**:1–20 DOI 10.3389/fpls.2014.00105.

Battaglia M, Covarrubias AA. 2013. Late embryogenesis abundant (LEA) proteins in legumes. *Frontiers in Plant Science* **4**:190 DOI 10.3389/fpls.2013.00190.

Battaglia M, Olvera-Carrillo Y, Garciarrubio A, Campos F, Covarrubias AA. 2008. The enigmatic LEA proteins and other hydrophilins. *Plant Physiology* **148(1)**:6–24 DOI 10.1104/pp.108.120725.

Bernarducci E, Schwindinger WF, Hughey JL, Krogh-Jespersen K, Schugar HJ. 1981. Electronic spectra of copper(II)-imidazole and copper(II)-pyrazole chromophores. *Journal of the American Chemical Society* **103(7)**:1686–1691 DOI 10.1021/ja00397a017.

Bocharova OV, Breydo L, Salnikov VV, Baskakov IV. 2005. Copper(II) inhibits in vitro conversion of prion protein into amyloid fibrils. *Biochemistry* **44(18)**:6776–6787 DOI 10.1021/bi050251q.

Bonda DJ, Lee HG, Blair JA, Zhu X, Perry G, Smith MA. 2011. Role of metal dyshomeostasis in Alzheimer's disease. *Metallomics* **3(3)**:267–270 DOI 10.1039/c0mt00074d.

Brautigam CA, Zhao H, Vargas C, Keller S, Schuck P. 2016. Integration and global analysis of isothermal titration calorimetry data for studying macromolecular interactions. *Nature Protocols* **11(5)**:882–894 DOI 10.1038/nprot.2016.044.

Bremer A, Wolff M, Thalhammer A, Hincha DK. 2017. Folding of intrinsically disordered plant LEA proteins is driven by glycerol-induced crowding and the presence of membranes. *FEBS Journal* **284(6)**:919–936 DOI 10.1111/febs.14023.

Breydo L, Uversky VN. 2011. Role of metal ions in aggregation of intrinsically disordered proteins in neurodegenerative diseases. *Metallomics* **3(11)**:1163 DOI 10.1039/c1mt00106j.

Bryce GF, Roeske RW, Gurd RN. 1966. L-histidine-containing peptides as models for the interaction of copper (II) and nickel (II) ions with sperm whale apomyoglobin. *Journal of Biological Chemistry* **241**:1072–1080.

Campos F, Guillén G, Reyes JL, Covarrubias AA. 2011. A general method of protein purification for recombinant unstructured non-acidic proteins. *Protein Expression and Purification* **80(1)**:47–51 DOI 10.1016/j.pep.2011.06.007.

Chakrabortee S, Boschetti C, Walton LJ, Sarkar S, Rubinsztein DC, Tunnacliffe A. 2007. Hydrophilic protein associated with desiccation tolerance exhibits broad protein stabilization

function. *Proceedings of the National Academy of Sciences of the United States of America* **104(46)**:18073–18078 DOI 10.1073/pnas.0706964104.

Chekmeneva E, Prohens R, Díaz-Cruz JM, Ariño C, Esteban M. 2008. Thermodynamics of Cd^{2+} and Zn^{2+} binding by the phytochelatin (γ-Glu-Cys)$_4$-Gly and its precursor glutathione. *Analytical Biochemistry* **375(1)**:82–89 DOI 10.1016/j.ab.2008.01.008.

Cuevas-Velazquez CL, Reyes JL, Covarrubias AA. 2017. Group 4 late embryogenesis abundant proteins as a model to study intrinsically disordered proteins in plants. *Plant Signaling & Behavior* **12(7)**:e1343777 DOI 10.1080/15592324.2017.1343777.

Cuevas-Velazquez CL, Saab-Rincón G, Reyes JL, Covarrubias AA. 2016. The unstructured N-terminal region of arabidopsis group 4 late embryogenesis abundant (LEA) proteins is required for folding and for chaperone-like activity under water deficit. *Journal of Biological Chemistry* **291(20)**:10893–10903 DOI 10.1074/jbc.M116.720318.

DalCorso G, Manara A, Piasentin S, Furini A. 2014. Nutrient metal elements in plants. *Metallomics* **6(10)**:1770–1788 DOI 10.1039/C4MT00173G.

Dure L, Pyle JB, Chlan CA, Baker JC, Galau GA. 1983. Developmental biochemistry of cottonseed embryogenesis and germination-XVII. Developmental expression of genes for the principal storage proteins. *Plant Molecular Biology* **2**:199–206 DOI 10.1007/BF01578379.

Garay-Arroyo A, Colmenero-Flores JM, Garciarrubio A, Covarrubias AA. 2000. Highly hydrophilic proteins in prokaryotes and eukaryotes are common during conditions of water deficit. *Journal of Biological Chemistry* **275(8)**:5668–5674 DOI 10.1074/jbc.275.8.5668.

Garnett AP, Viles JH. 2003. Copper binding to the octarepeats of the prion protein. *Journal of Biological Chemistry* **278(9)**:6795–6802 DOI 10.1074/jbc.M209280200.

Gusman H, Lendenmann U, Grogan J, Troxler RF, Oppenheim FG. 2001. Is salivary histatin 5 a metallopeptide? *Biochimica et Biophysica Acta (BBA)–Protein Structure and Molecular Enzymology* **1545(1–2)**:86–95 DOI 10.1016/S0167-4838(00)00265-X.

Hand SC, Menze MA, Toner M, Boswell L, Moore D. 2011. LEA proteins during water stress: not just for plants anymore. *Annual Review of Physiology* **73(1)**:115–134 DOI 10.1146/annurev-physiol-012110-142203.

Hara M, Fujinaga M, Kuboi T. 2004. Radical scavenging activity and oxidative modification of citrus dehydrin. *Plant Physiology and Biochemistry* **42(7–8)**:657–662 DOI 10.1016/j.plaphy.2004.06.004.

Hara M, Fujinaga M, Kuboi T. 2005. Metal binding by citrus dehydrin with histidine-rich domains. *Journal of Experimental Botany* **56(420)**:2695–2703 DOI 10.1093/jxb/eri262.

Hara M, Kondo M, Kato T. 2013. A KS-type dehydrin and its related domains reduce Cu-promoted radical generation and the histidine residues contribute to the radical-reducing activities. *Journal of Experimental Botany* **64(6)**:1615–1624 DOI 10.1093/jxb/ert016.

Hara M, Monna S, Murata T, Nakano T, Amano S, Nachbar M, Wätzig H. 2016. The Arabidopsis KS-type dehydrin recovers lactate dehydrogenase activity inhibited by copper with the contribution of His residues. *Plant Science* **245**:135–142 DOI 10.1016/j.plantsci.2016.02.006.

Hara M, Shinoda Y, Tanaka Y, Kuboi T. 2009. DNA binding of citrus dehydrin promoted by zinc ion. *Plant Cell & Environment* **32(5)**:532–541 DOI 10.1111/j.1365-3040.2009.01947.x.

Hincha DK, Thalhammer A. 2012. LEA proteins: IDPs with versatile functions in cellular dehydration tolerance. *Biochemical Society transactions* **40**:1000–1003 DOI 10.1042/BST20120109.

Jin F, Yu C, Lai L, Liu Z. 2013. Ligand clouds around protein clouds: a scenario of ligand binding with intrinsically disordered proteins. *PLOS Computational Biology* **9(10)**:e1003249 DOI 10.1371/journal.pcbi.1003249.

Keller S, Vargas C, Zhao H, Piszczek G, Brautigam CA, Schuck P. 2012. High-precision isothermal titration calorimetry with automated peak-shape analysis. *Analytical Chemistry* **84(11)**:5066–5073 DOI 10.1021/ac3007522.

Koag MC, Wilkens S, Fenton RD, Resnik J, Vo E, Close TJ. 2009. The K-segment of maize DHN1 mediates binding to anionic phospholipid vesicles and concomitant structural changes. *Plant Physiology* **150(3)**:1503–1514 DOI 10.1104/pp.109.136697.

Kovács D, Agoston B, Tompa P. 2008. Disordered plant LEA proteins as molecular chaperones. *Plant Signaling & Behavior* **3(9)**:710–713 DOI 10.1104/pp.108.118208.

Kranner I, Colville L. 2011. Metals and seeds: biochemical and molecular implications and their significance for seed germination. *Environmental and Experimental Botany* **72(1)**:93–105 DOI 10.1016/j.envexpbot.2010.05.005.

Krüger C, Berkowitz O, Stephan UW, Hell R. 2002. A Metal-binding Member of the Late Embryogenesis Abundant Protein Family Transports Iron in the Phloem of *Ricinus communis* L. *Journal of Biological Chemistry* **277**:25062–25069 DOI 10.1074/jbc.M201896200.

Letelier ME, Lepe AM, Faúndez M, Salazar J, Marín R, Aracena P, Speisky H. 2005. Possible mechanisms underlying copper-induced damage in biological membranes leading to cellular toxicity. *Chemico-Biological Interactions* **151(2)**:71–82 DOI 10.1016/j.cbi.2004.12.004.

Liu G, Liu K, Gao Y, Zheng Y. 2017. Involvement of C-terminal histidines in soybean PM1 protein oligomerization and Cu^{2+} binding. *Plant and Cell Physiology* **58(6)**:1018–1029 DOI 10.1093/pcp/pcx046.

Liu Y, Wang L, Xing X, Sun L, Pan J, Kong X, Zhang M, Li D. 2013. ZmLEA3, a multifunctional group 3 LEA protein from maize (*Zea mays* L.), is involved in biotic and abiotic stresses. *Plant and Cell Physiology* **54(6)**:944–959 DOI 10.1093/pcp/pct047.

Liu G, Xu H, Zhang L, Zheng Y. 2011. Fe binding properties of two soybean (*Glycine max* L.) LEA4 proteins associated with antioxidant activity. *Plant and Cell Physiology* **52(6)**:994–1002 DOI 10.1093/pcp/pcr052.

Mo ZY, Zhu YZ, Zhu HL, Fan JB, Chen J, Liang Y. 2009. Low micromolar zinc accelerates the fibrillization of human Tau via bridging of Cys-291 and Cys-322. *Journal of Biological Chemistry* **284(50)**:34648–34657 DOI 10.1074/jbc.M109.058883.

Nunes AM, Zavitsanos K, Malandrinos G, Hadjiliadis N. 2010. Coordination of Cu^{2+} and Ni^{2+} with the histone model peptide of H2B N-terminal tail (1–31 residues): a spectroscopic study. *Dalton Transactions* **39(18)**:4369 DOI 10.1039/b927157k.

Olvera-Carrillo Y, Campos F, Reyes JL, Garciarrubio A, Covarrubias AA. 2010. Functional analysis of the group 4 late embryogenesis abundant proteins reveals their relevance in the adaptive response during water deficit in arabidopsis. *Plant Physiology* **154(1)**:373–390 DOI 10.1104/pp.110.158964.

Olvera-Carrillo Y, Reyes JL, Covarrubias AA. 2011. Late embryogenesis abundant proteins. *Plant Signaling & Behavior* **6(4)**:586–589 DOI 10.4161/psb.6.4.15042.

Otegui MS. 2002. Developing seeds of arabidopsis store different minerals in two types of vacuoles and in the endoplasmic reticulum. *Plant Cell Online* **14(6)**:1311–1327 DOI 10.1105/tpc.010486.

Peisach J, Blumberg WE. 1974. Structural implications derived from the analysis of electron paramagnetic resonance spectra of natural and artificial copper proteins. *Archives of Biochemistry and Biophysics* **165(2)**:691–708 DOI 10.1016/0003-9861(74)90298-7.

Ravet K, Pilon M. 2013. Copper and iron homeostasis in plants: the challenges of oxidative stress. *Antioxidants & Redox Signaling* **19(9)**:919–932 DOI 10.1089/ars.2012.5084.

Reyes JL, Campos F, Wei H, Arora R, Yang Y, Karlson DT, Covarrubias AA. 2008. Functional dissection of hydrophilins during in vitro freeze protection. *Plant, Cell & Environment* **31(12)**:1781–1790 DOI 10.1111/j.1365-3040.2008.01879.x.

Reyes JL, Rodrigo MJ, Colmenero-Flores JM, Gil JV, Garay-Arroyo A, Campos F, Salamini F, Bartels D, Covarrubias AA. 2005. Hydrophilins from distant organisms can protect enzymatic activities from water limitation effects in vitro. *Plant, Cell and Environment* **28(6)**:709–718 DOI 10.1111/j.1365-3040.2005.01317.x.

Rivera-Najera LY, Saab-Rincón G, Battaglia M, Amero C, Pulido NO, García-Hernández E, Solórzano RM, Reyes JL, Covarrubias AA. 2014. A group 6 late embryogenesis abundant protein from common bean is a disordered protein with extended helical structure and oligomer-forming properties. *Journal of Biological Chemistry* **289(46)**:31995–32009 DOI 10.1074/jbc.M114.583369.

Roberts JK, DeSimone NA, Lingle WL, Dure L III. 1993. Cellular concentrations and uniformity of cell-type accumulation of two lea proteins in cotton embryos. *Plant Cell* **5(7)**:769–780 DOI 10.1105/tpc.5.7.769.

Sacco C, Skowronsky RA, Gade S, Kenney JM, Spuches AM. 2012. Calorimetric investigation of copper(II) binding to Aβ peptides: thermodynamics of coordination plasticity. *JBIC Journal of Biological Inorganic Chemistry* **17(4)**:531–541 DOI 10.1007/s00775-012-0874-3.

Saumonneau A, Laloi M, Lallemand M, Rabot A, Atanassova R. 2012. Dissection of the transcriptional regulation of grape ASR and response to glucose and abscisic acid. *Journal of Experimental Botany* **63(3)**:1495–1510 DOI 10.1093/jxb/err391.

Senthil-Kumar M, Udayakumar M. 2006. High-throughput virus-induced gene-silencing approach to assess the functional relevance of a moisture stress-induced cDNA homologous to *lea*4. *Journal of Experimental Botany* **57(10)**:2291–2302 DOI 10.1093/jxb/erj200.

Shih M, Hsieh T, Lin T, Hsing Y, Hoekstra FA. 2010. Characterization of two soybean (*Glycine max* L.) LEA IV proteins by circular dichroism and fourier transform infrared spectrometry. *Plant and Cell Physiology* **51(3)**:395–407 DOI 10.1093/pcp/pcq005.

Soulages JL, Kim K, Walters C, Cushman JC. 2002. Temperature-induced extended helix/random coil transitions in a group 1 late embryogenesis-abundant protein from soybean. *Plant Physiology* **128(3)**:822–832 DOI 10.1104/pp.010521.

Stetefeld J, McKenna SA, Patel TR. 2016. Dynamic light scattering: a practical guide and applications in biomedical sciences. *Biophysical Reviews* **8(4)**:409–427 DOI 10.1007/s12551-016-0218-6.

Tomasso ME, Tarver MJ, Devarajan D, Whitten ST. 2016. Hydrodynamic radii of intrinsically disordered proteins determined from experimental polyproline II propensities. *PLOS Computational Biology* **12(1)**:e1004686 DOI 10.1371/journal.pcbi.1004686.

Uversky VN, Li J, Fink AL. 2001. Metal-triggered structural transformations, aggregation, and fibrillation of human α-synuclein: A possible molecular link between parkinson's disease and heavy metal exposure. *Journal of Biological Chemistry* **276**:44284–44296 DOI 10.1074/jbc.M105343200.

Wiedemann C, Bellstedt P, Görlach M. 2013. CAPITO-a web server-based analysis and plotting tool for circular dichroism data. *Bioinformatics* **29(14)**:1750–1757 DOI 10.1093/bioinformatics/btt278.

Zhao H, Piszczek G, Schuck P. 2015. SEDPHAT-a platform for global ITC analysis and global multi-method analysis of molecular interactions. *Methods* **76**:137–148 DOI 10.1016/j.ymeth.2014.11.012.